Journal of Applied Polymer Science

Electrospun Polystyrene Coatings with Tunable Wettability

Negar Ghochaghi, Adetoun Taiwo, Matthew Winkel, Brandon Dodd, Karla Mossi, Gary Tepper
Department of Mechanical and Nuclear Engineering, Virginia Commonwealth University, Richmond, Virginia 23284
Correspondence to: G. C. Tepper (E-mail: gctepper@vcu.edu)

ABSTRACT: Hydrophobic materials with tunable wettability were developed by electrospinning aligned polystyrene (PS) fibers onto the surface of a unimorph composite piezoelectric substrate. An electric field was used to modify the curvature of the substrate resulting in a corresponding change in the morphology of the electrospun coating. Contact angle measurements were performed on droplets deposited onto the surface before and after application of the electric field. The water droplet contact angle was observed to change in response to the applied voltage. Contact angle measurements were performed as a function of surface fiber density and suggest that the change in contact angle is caused by a transition from Wenzel to Cassie–Baxter wetting. © 2014 Wiley Periodicals, Inc. J. Appl. Polym. Sci. **2015**, *132*, 41592.

KEYWORDS: electrospinning; morphology; polystyrene

Received 2 June 2014; accepted 2 October 2014
DOI: 10.1002/app.41592

INTRODUCTION

Hydrophobic (i.e., water repellent) materials including oils, fats, silicones and fluoropolymers (e.g., Teflon) are common and exhibit a water droplet contact angle exceeding 90°. A hydrophobic material with microstructure or roughness can exhibit a significant enhancement in the water droplet contact angle and these surfaces are normally called superhydrophobic.[1,2] Superhydrophobic surfaces exist in nature (e.g., the Lotus leaf) and have also been synthesized using a wide variety of techniques.[3–5] Interest in superhydrophobic surfaces is driven by their potential use in applications ranging from drag reduction to self-cleaning surfaces and medical devices. The wettability of a superhydrophobic surface is usually fixed and determined by the chemical properties of the surface material and the surface microstructure. Several methods have been developed to control surface wettability, and typically involve chemical modification.[6–15] This article introduces electroactivation of a smart material as a new means of modifying surface wettability.[16–19]

Smart materials (e.g., piezoelectrics, ferrofluids, shape memory alloys) have one or more properties that can change in response to external stimuli such as an electric or magnetic field. A smart hydrophobic or smart superhydrophobic material will change wettability in response to an external stimuli and the ability to actively tune the wettability of a surface could lead to the development of new devices such as microfluidic switches, sensors, flow control and chemical separations systems. Several studies have shown that the wettability of a surface can be changed by modifying the surface chemistry or electrochemistry.[20–23] However, surface chemical modification using optical or thermal activation, pH changes or electrolytes is limited to specific surface materials and/or water droplet properties and, therefore, may be difficult to apply broadly. Active and reversible tuning of surface morphology (in contrast to the surface chemistry) is challenging because of the need to mobilize surface structures rather than molecules, but could potentially be applied to a much broader range of materials. One group modified the wettability of a Teflon film by manually stretching the film and increasing its dimensions by up to 200%.[16] While the Teflon film used in this study is not a smart material, the study demonstrated that dimensional changes in a material could result in changes in wettability. Another study showed that the wettability of an electrospun coating incorporating magnetic particles could be modified through the application of an external magnetic field.[24]

Piezoelectric materials, a group of smart materials that convert electrical energy into mechanical energy, could potentially be used to change surface microstructure and hydrophobicity. However, piezoelectric constants are typically in the range of 10^{-10} m V^{-1} so that the surface strain produced from even very large electric fields is insufficient to appreciably affect surface microstructure and wettability. A unimorph is a composite structure (e.g., a cantilever) with one active piezoelectric component and one inactive component. Unlike pure piezoelectric materials, unimorph composites can deform significantly in response to an electric field and have been used to construct actuators for applications such as flow control and

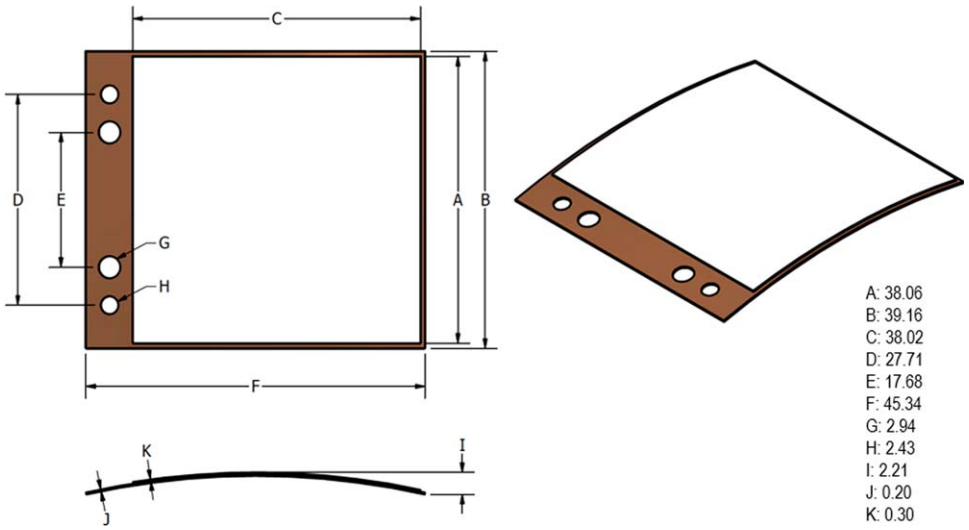

Figure 1. Thin Piezoelectric Unimorph Actuator (Dimensions in mm). (Reproduced from http://www.faceinternational.com). [Color figure can be viewed in the online issue, which is available at wileyonlinelibrary.com.]

acoustics.[25–30] This article describes our preliminary work to develop compliant hydrophobic and superhydrophobic electrospun polymer coatings on piezoelectric unimorph composite substrates that can exhibit a field-induced change in geometry and a corresponding change in wettability. The main aim of this project is to investigate the tunability of the wetting behavior of a hydrophobic coating through a voltage-induced mechanical process. The assumption is that understanding of this process would facilitate the design of a superhydrophobic material that can be tuned with the aid of a smart material. The hydrophobic coating was produced by electrospinning polystyrene (PS) fibers onto smart substrates (piezoelectric unimorphs). Wettability was determined by measuring the contact angles made by water droplets applied onto the fiber-coated substrate.[31] Polystyrene was selected for this study because it is a common, low-cost hydrophobic polymer that is readily available and well-studied in the context of electrospinning.[32,33]

Electrospinning is a technique that uses an electric field to draw polymer fibers from a solution.[34–36] Electrospun fibers can be readily deposited onto a variety of substrates and superhydrophobic surfaces of hydrophobic polymers such as polystyrene have been developed using this method.[37–39] Normally, because electrospun fibers are electrically charged and mechanically unstable, the resulting surfaces consist of a mat of randomly oriented fibers. However, several methods have been developed to reduce the fiber instability resulting in electrospun surfaces of highly aligned polymer fibers.[33,35,40]

The unimorph composite substrates used consisted of rectangular surfaces of the dimensions shown in Figure 1. These devices have layers of stainless steel, lead zirconate titanate (PZT), and Aluminum.[41] PZT is a common piezoceramic material and is physically rugged, chemically inert and relatively inexpensive. The importance of using this kind of composite substrate is that it allows for an electric field induced change in surface curvature, which consequently alters fiber morphology. Our initial results show that it is possible to actively change surface wettability on polymer-coated unimorph composites using an applied electric field.

EXPERIMENTAL

The electrospinning apparatus and methods used in these experiments have been described in detail elsewhere.[33,38–40] Polystyrene (average molecular weight ~350,000) solutions were made by dissolving the solute at concentrations ranging from 18 to 25% by weight in a toluene/dimethylformamide or toluene/tetrahydrofuran solvent mixture as illustrated in Table I.

Each solution was placed into a hypodermic syringe and a positive voltage of 5.5 kV was placed on the syringe tip with respect to a grounded target. The distance between the syringe tip and the grounded target was 7.5–10 cm and the syringe pump infusion rate was set for each solution as shown in Table II. To deposit aligned fibers a rotating drum was used as the grounded target. The unimorph substrate was placed on the drum and the rotation speed was ~1200 rpm. To deposit random fibers, the unimorph substrate was placed on a stationary grounded collecting electrode. To characterize the samples, a Hitachi SU-70 scanning electron microscope (SEM) was used. Fiber diameters were obtained from SEM images taken at the center of the unimorph using ImageJ. The average diameter of fibers along a line in the SEM image was calculated. Figure 2(a) is an SEM image showing a typical mat of randomly oriented polystyrene fibers with an average diameter of 3.96 ± 0.20 μm. Figure 2(b)

Table I. Polystyrene Solutions Used in this Study

% Concentration polystyrene	Solvent
20%	Toluene/dimethylformamide <7 : 3>
18%	Toluene/tetrahydrofuran <7 : 3>
20%	Toluene/tetrahydrofuran <7 : 3>
25%	Toluene/tetrahydrofuran <7 : 3>

Table II. Table Showing Results for Changes in WCA of Polystyrene Fibers due to 400–500 V Applied to Unimorph Substrate

Solvent components	% PS	Electrospinning infusion rate (μL min^{-1})	Electrospun fiber deposition time (min)	Average fiber Diameter (μm)	Average ΔWCA
70%Toluene30% DMF	20	2.0	5	2.609 ± 0.120	9.6 ± 1.90
70%Toluene30% THF	25	2.5	5	2.097 ± 0.079	7.2 ± 1.20
70%Toluene30% THF	25	2.5	1-2	2.097 ± 0.079	2.5 ± 0.92
70%Toluene30% THF	18	0.5-1.0	10	0.583 ± 0.077	3.5 ± 1.37

is an SEM image showing the aligned polystyrene fibers with an average diameter of 2.609 ± 0.120 μm. Both coatings are on a unimorph substrate. The smaller diameter of the aligned fibers is the result of the rotational motion of the collector.

The contact angle of water droplets deposited onto the center of the polymer-coated substrate was measured on both sides of each droplet before and after electro-activation of the substrate using a Ramé-Hart Model 100-25A Advanced Goniometer. Each contact angle represents the average of measurements taken from both sides of the droplet. Immediately after a droplet of water was placed on the fiber coating and an initial image captured, the unimorph substrate was electro-activated by applying 400–500VDC through leads attached between the front and back surfaces of the unimorph using a FACE TD-2 Test Driver™ high power supply and function generator. This produced a macroscopic change in the substrate curvature and a corresponding deformation of the fiber coating.

For randomly oriented fibers, no statistically significant change in contact angle was observed after electro-activation of the substrate. In the case of aligned fibers, a modest, but statistically significant and reproducible change in the water droplet contact angle with substrate electro-activation was observed, but only when the fibers were aligned in a direction orthogonal to the direction of substrate curvature. Figure 3 illustrates the direction of fiber alignment relative to that of electroactivation.

RESULTS AND DISCUSSION

The experiments described above in which droplet contact angles were measured before and after electroactivation of the coating substrate are discussed in this section. Results from the coating of 20% polystyrene dissolved in toluene and DMF, showed a decrease in contact angle ranging from 6.5° to 15.1° with an average decrease of 9.6° + 1.9° at 90% confidence. Figure 4(a,b) show photographs of a water droplet on an aligned fiber coating before (a) and after (b) the application of the applied voltage. The water droplet contact angle in Figure 4 decreased from 142.8° to 130.5° (12.3° change) with applied voltage.

The average values of the changes in water contact angles (WCA) due to electroactivation from experiments using different solutions are summarized in Table II below. The standard deviation values in Table II were calculated using "student *t* distribution" at a 90% confidence interval.[42]

The observed change in water droplet contact angle with substrate curvature is due to a change in the wetting state of the droplet in contact with the surface. The Cassie–Baxter wetting state occurs on heterogeneous surfaces exhibiting both a wetting phase (the hydrophobic polymer) and a non-wetting phase (the air between the fibers). In the Cassie–Baxter state, because the water droplet is only in contact with the wetting phase, very large contact angles can be achieved and depends on the fraction of the solid surface area in contact with the liquid. Mechanical changes in the surface morphology that modify the fraction of the solid surface area wet by the liquid will change the water droplet contact angle.

The Cassie–Baxter equation relates the contact angle on the heterogeneous (i.e., air-polymer) surface (θ^*) to the contact angle on the smooth polymer surface (θ) as:

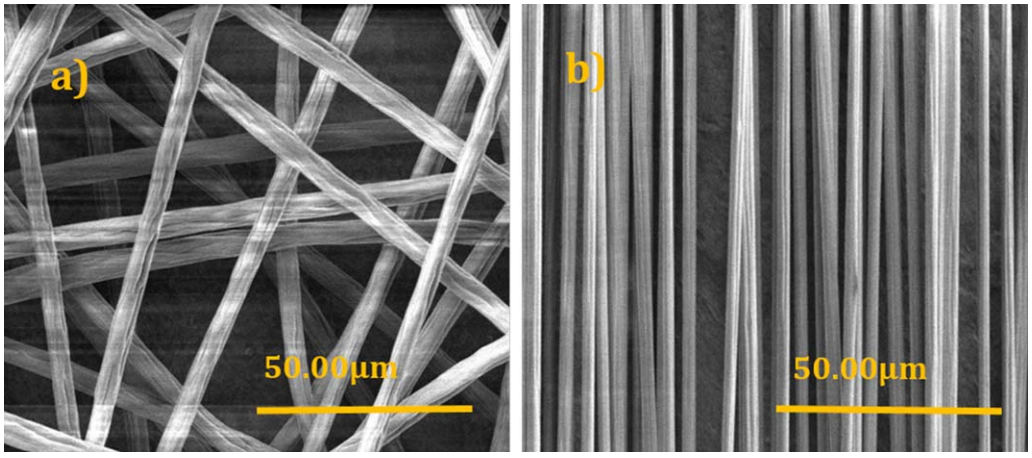

Figure 2. (a) random and (b) aligned polystyrene fibers electrospun onto a piezoelectric unimorph substrate for 5 min. [Color figure can be viewed in the online issue, which is available at wileyonlinelibrary.com.]

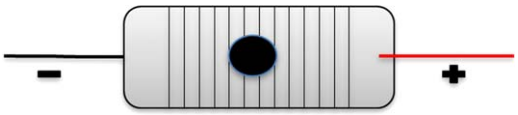

Figure 3. Diagram illustrating direction of fiber alignment, droplet location and contact points for application of electric field (note that image is not drawn to scale). [Color figure can be viewed in the online issue, which is available at wileyonlinelibrary.com.]

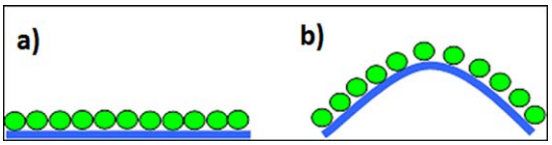

Figure 5. Cross-sectional schematic diagram illustrating the influence of substrate curvature on fiber density. [Color figure can be viewed in the online issue, which is available at wileyonlinelibrary.com.]

$$\cos(\theta^*) = f\ (\cos(\theta) + 1) - 1 \quad (1)$$

where f is the fraction of solid surface area wet by the liquid. Because the contact angle of water droplets on a smooth polystyrene surface is ~90°, eq. (1) can be used to estimate the fraction of solid surface area wet by the liquid for the electrospun polystyrene surfaces of Figure 4. According to eq. (1), $f = 0.20$ for the contact angle data shown in Figure 4(a) and $f = 0.35$ for the contact angle data shown in Figure 4(b). That is, according to the Cassie–Baxter equation, a 75% increase in f would be necessary to explain the observed 12.3° change in water droplet contact angle with surface curvature. This is not possible given the relatively small change in overall substrate curvature. Therefore, a different mechanism must be responsible for the observed change in water droplet contact angle with substrate curvature. Electrowetting is ruled out as the cause for the observed changes in water droplet contact angle with applied voltage since no effect was observed unless the polystyrene fibers were oriented in a direction orthogonal to the direction of surface curvature. Electrowetting effects would be insensitive to the fiber orientation.

The piezoelectric substrate has been well characterized and its electromechanical properties and dimensional changes are well known.[26,28–30] At an applied voltage of 500 V the maximum amount of substrate strain is about 1×10^{-3} m m^{-1} at the center where the water droplet is placed.[27] While the amount of surface strain is relatively small, the composite piezoelectric unimorph substrates used in this work undergo a significant macroscopic change in overall shape and these materials have been used to produce synthetic air jets and in flow control applications.[25] The amount of substrate deformation due to the applied electric field is on the order of millimeters and can be seen with the unaided eye. The edges of the substrate were unconstrained during the application of the electric field and the rectangular disc deformed from a state of maximum curvature to a state of minimum curvature causing the dimension (I) in Figure 1 to decrease from 2.2 mm to close to 0 mm.

For the aligned fiber coating, the electrospinning apparatus lays down a specific number of fibers across the substrate per unit length. When the substrate deforms, the compliant fibers will conform to the shape of the underlying substrate. No electric field was applied to the substrate during fiber deposition and it was, therefore, in a state of maximum curvature ($I = 2.2$ mm). Electroactivation caused the substrate to flatten ($I = 0$ mm). Because the fibers are deposited in a direction orthogonal to the direction of substrate curvature, the fiber density will increase slightly as the substrate curvature decreases as illustrated schematically in Figure 5. The fact that no change in wettability was observed for randomly oriented fiber coatings or for coatings with fibers aligned in the direction of substrate curvature supports this proposed mechanism and also rules out surface curvature itself as the mechanism responsible for the observed change in wettability.

The effect of fiber surface density on the water contact angle was investigated by depositing fibers from a 25 wt % polystyrene solution at deposition times ranging from 2 to 40 min. Figure 6 is a plot of the water droplet contact angle as a function of deposition time. Statistical analysis was done using t distribution, specifically to calculate the confidence interval where $n = 12$ for deposition times 2–10 min and $n = 6$ for 15–40 min (except for the sample with 25-min deposition where $n = 5$). six

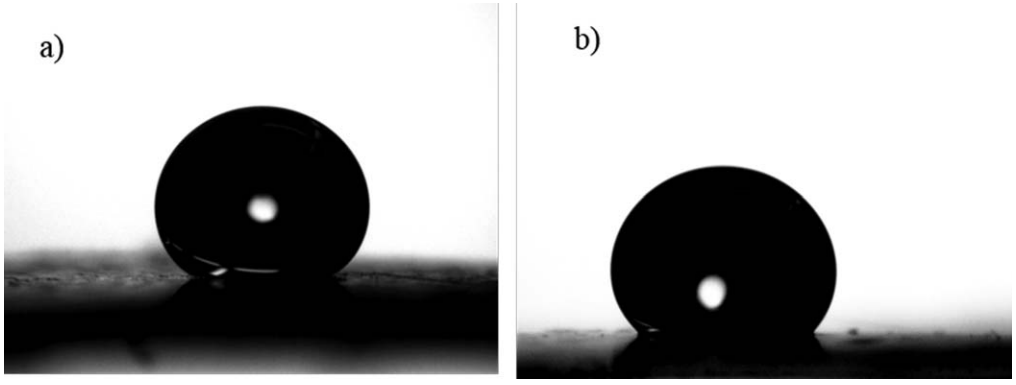

Figure 4. Water droplet on aligned coating derived from 20 wt % polystyrene dissolved in 7 : 3 Toluene/DMF solvent mixture spun for 5 min (a) before electroactivation of substrate and (b) after electroactivation of substrate.

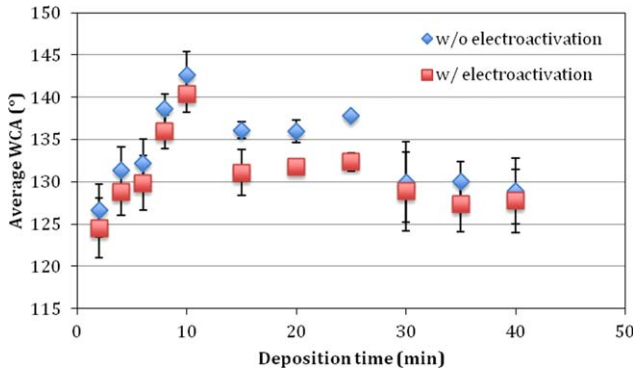

Figure 6. Average water droplet contact angles versus fiber deposition time for 25%PS. [Color figure can be viewed in the online issue, which is available at wileyonlinelibrary.com.]

drops were placed on each unimorph across the center of the surface. For each deposition time in Figure 6, the six drops are represented by an average value shown by a dot on the plot. Error bars were placed using *t* values.

The water droplet contact angle initially increases rapidly with deposition time from ~127° at 2 min to ~143° at 10 min. After ten minutes of deposition, the water droplet contact angle begins to gradually decrease with increasing deposition time, reaching a value of about 129° at 40 min. The Cassie–Baxter equation was used to calculate the fraction of solid in contact with the liquid *(f)* at each deposition (this calculation assumes a Cassie–Baxter surface wetting state). The results are shown in Figure 7.

The fraction of water in contact with the solid (polymer) is expected to increase with increasing polymer deposition time since increasing the deposition time increases the fiber density on the surface. However, below a deposition time of 10 min, the fraction of water in contact with the polymer as determined from the Cassie–Baxter equation decreases with increasing deposition time. The surface wetting state for deposition times <10 min is, therefore, inconsistent with the Cassie–Baxter equation. We conclude that, below a deposition time of 10 min, the large average spacing between the fibers results in some amount of

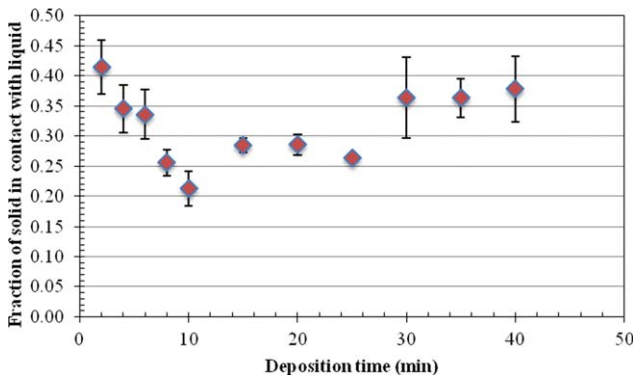

Figure 7. Plot showing the fraction of solid in contact with the liquid (*f* parameter) with respect to fiber deposition time for 25%PS, without electroactivation of substrate. [Color figure can be viewed in the online issue, which is available at wileyonlinelibrary.com.]

Wenzel wetting. In the Wenzel state, the water droplet will penetrate into the air region between the fibers. As the deposition time increases, the average fiber spacing decreases causing a transition from the Wenzel state to the Cassie–Baxter state. After 10 min of deposition, the surface is primarily in the Cassie–Baxter wetting mode and the measured contact angle decreases with an increase in the area fraction, *f*, as predicted from the Cassie–Baxter equation.

CONCLUSIONS

The changes in water droplet contact angle with surface curvature were observed on surfaces with deposition times <10 min. Based on the measurements of contact angle, versus deposition time, we conclude that these surfaces exhibit a combination of both Wenzel wetting and Cassie–Baxter wetting and that there is a transition from the Wenzel state to the Cassie–Baxter state with increasing fiber density. Therefore, the observed decrease in water droplet contact angle with applied voltage is likely due to a transition from Wenzel wetting to Cassie–Baxter wetting with decreasing surface curvature.

While these initial results show only a modest change in wettability with applied voltage, we believe much larger changes should be possible through optimization of the coating and substrate properties. A more detailed experimental and theoretical analysis of these geometry-induced changes in surface wetting is needed and future studies should include a comprehensive model of the substrate and fiber geometry as a function of applied electric field and include different polymers and fiber diameters.

REFERENCES

1. Lafuma, A.; Quere, D. *Nat. Mater.* **2003**, *2*, 457.
2. Erbil, H. Y.; Demirel, A. L.; Avci, Y.; Mert, O. *Science* **2003**, *299*, 1377.
3. Feng, X. J.; Jiang, L. *Adv. Mater.* **2006**, *18*, 3063.
4. Bixler, G. D.; Bhushan, B. *Soft Matter* **2012**, *8*, 11271.
5. Dorrer, C.; Rühe, J. *Soft Matter* **2009**, *5*, 51.
6. Ma, M.; Hill, R. M. *Curr. Opin. Colloid Interface Sci.* **2006**, *11*, 193.
7. Shi, Y.; Wang, Y.; Feng, X.; Yue, G.; Yang, W. *Appl. Surf. Sci.* **2012**, *258*, 8134.
8. Zhang, X.; Shi, F.; Nia, J.; Jiang, Y.; Wang, Z. *J. Mater. Chem.* **2008**, *18*, 621.
9. Ebert, D.; Bhushan, B. *J. Colloid Interface Sci.* **2012**, *384*, 182.
10. Li, X.; Ding, B.; Lin, J.; Yu, J.; Sun, G. *J. Phys. Chem. C* **2009**, *113*, 20452.
11. Lin, J.; Cai, Y.; Wang, X.; Ding, B.; Yu, J.; Wang, M. *Nanoscale* **2011**, *3*, 1258.
12. Roach, P.; Shirtcliff, N. J.; Newton, M. I. *Soft Matter* **2008**, *4*, 224.
13. Kim, E.-K.; Kim, J. Y.; Kim, S. S. *J. Solid State Chem.* **2013**, *197*, 23.

14. Men, X.; Zhang, Z.; Yang, J.; Zhu, X.; Kun, W.; Jiang, W. N. *J. Chem.* **2011**, *35*, 881.
15. He, Y.; Jiang, C.; Yin, H.; Yuan, W. *Appl. Surf. Sci.* **2011**, *257*, 7689.
16. Zhang, J.; Han, Y. *Macromol. Rapid Commun.* **2004**, *25*, 1105.
17. Zheng, J.; He, A.; Li, J.; Xu, J.; Charles, H. C. *Polymer* **2006**, *47*, 7095.
18. Wu, H.; Zhang, R.; Sun, R.; Lin, D.; Sun, Z.; Pan, W.; Downs, P. *Soft Matter* **2008**, *4*, 2429.
19. Xie, Z.; Buschle-Diller, G. *J. Appl. Polym. Sci.* **2011**, *122*, 1219.
20. Abbott, S.; Ralston, J.; Reynolds, G.; Hayes, R. *Langmuir* **1999**, *15*, 8923.
21. Jones, D. M.; Smith, J. R.; Huck, W. T.; Alexander, C. *Adv. Mater.* **2002**, *14*, 1130.
22. Li, C.; Zhang, Y.; Ju, J.; Cheng, F.; Liu, M.; Jiang, L.; Yu, Y. *Adv. Funct. Mater.* **2012**, *22*, 760.
23. Yu, X.; Wang, Z.; Jiang, Y.; Shi, F.; Zhang, X. *Adv. Mater.* **2005**, *17*, 1289.
24. Ho, T.; Ghochaghi, N.; Tepper, G. C. *J. Appl. Polym. Sci.* **2013**, *130*, 2352.
25. Mane, P.; Mossi, K.; Rostami, A.; Bryant, R.; Castro, N. *J. Intell. Mater. Syst. Struct.* **2007**, *18*, 221.
26. Mossi, K.; Selby, G.; Bryant, R. *Mater. Lett.* **1998**, *35*, 39.
27. Bryant, R. G.; Mossi, K. M.; Robbins, J. A.; Bathel, B. F. *Integr. Ferroelectr.* **2005**, *71*, 267.
28. Wise, S. A. *Sens. Actuat. A Phys.* **1998**, *69*, 33.
29. Mulling, J.; Usher, T.; Dessent, B.; Palmer, J.; Franzon, P.; Grant, E.; Kingon, A. *Sens. Actuat. A Phys.* **2001**, *94*, 19.
30. Yoon, K. J.; Park, K. H.; Lee, S. K.; Goo, N. S.; Park, H. C. *Smart Mater. Struct.* **2004**, *13*, 459.
31. Taiwo, A. O. M.S. Thesis **2013**, Virginia Commonwealth University.
32. Wanatong, L.; Sirivat, A.; Supaphol, P. *Polym. Int.* **2004**, *53*, 1851.
33. Sarkar, S.; Deevi, S. C.; Tepper, G. *Macromol. Rapid Commun.* **2007**, *28*, 1034.
34. Huang, Z. M.; Zhang, Y. Z.; Kotaki, M.; Ramakrishna, S. *Compos. Sci. Technol.* **2003**, *63*, 2223.
35. Li, D.; Xia, Y. N. *Adv. Mater.* **2004**, *16*, 1151.
36. Stanger, J.; Tucker, N.; Stagier, M. *Rapra Rev. Rep.* **2005**, *16*, 6. (Smithers Rapra, Shrewsbury, Shropshire, GBR).
37. Nuraje, N.; Khan, W. S.; Lei, Y.; Ceylan, M.; Asmatulu, R. *J. Mater. Chem. A1* **2013**, *1*, 1929.
38. Samaha, M. A.; Ochanda, F. O.; Tafreshi, H. V.; Tepper, G. C.; Gad-el-Hak, M. *Rev. Sci. Instrum.* **2011**, *82*, 045109-1.
39. Emami, B.; Tafreshi, H. V.; Gad-el-Hak, M.; Tepper, G. C. *Appl. Phys. Lett.* **2011**, *98*, 2031061.
40. Ochanda, F. O.; Samaha, M. A.; Tafreshi, H. V.; Tepper, G. C.; Gad-el-Hak, M. *J. Appl. Polym. Sci.* **2012**, *123*, 1112.
41. Lawver, A. *Smart Mater. Bull.* **2001**, *2001*, 5.
42. Figliola, R. S.; Beasley, D. E. Theory and Design for Mechanical Measurements, 3rd ed.; Wiley: Hoboken, NJ, **2000**; Chapter 4, p 121.